

Journal of Applied Mathematics and Mechanics

# ZAMM

Zeitschrift für Angewandte Mathematik und Mechanik  
Founded by Richard von Mises in 1921

[www.zamm-journal.org](http://www.zamm-journal.org)

WILEY

REPRINT

# Stability analysis of some fully developed mixed convection flows in a vertical channel

M. Miklavčič\*

Department of Mathematics, Michigan State University, E. Lansing, MI 48824

Received 26 October 2014, revised 22 December 2014, accepted 1 February 2015

Published online 25 February 2015

**Key words** Instability, dual solution, mixed convection, viscous dissipation, passive.

**AMS Subject classification:** 35Q35, 35K58, 35P15, 76E15, 76R05, 80A20, 34B15, 34B09

Stability of fully developed mixed convection flows, with significant viscous dissipation, in a vertical channel bounded by isothermal plane walls having the same temperature and subject to pressure gradient is investigated. It is shown that one of the dual solutions is always unstable and that both are unstable when the total flow rate is big enough. The completely passive natural convection flow is shown to be unstable.

© 2015 WILEY-VCH Verlag GmbH & Co. KGaA, Weinheim

## 1 Introduction

Consider a fluid between two parallel vertical plates at a fixed temperature  $T_a$  and with no pressure gradient, except for the one due to gravity. One would expect the fluid to have temperature  $T_a$  and be at rest. However, various very reasonable models allow also a nontrivial solution. One of them was obtained in [6] and was called a completely passive natural convection. Another example of an unexpected channel flow can be found in [3]. In this case one wall is at rest and at a uniform temperature while the other wall is moving and insulated. When the other wall is at rest too, they [3] also found a nontrivial solution. Such paradoxes can lead one to question the modeling [9]. However, in [8] it was shown that for any given integer  $N$  one can find a boundary value problem based on exact Navier-Stokes equations with  $N$  solutions. Hence, multiple solutions do not have to be restricted to two, nor do they imply use of questionable approximations. It is often the stability analysis that clarifies their roles [7, 11].

The main purpose of this paper is to demonstrate instability of the completely passive natural convection and to show how this instability develops in a transition from the stable trivial solution. Various other published stationary solutions [1, 2] are on the transition path and their stability is discussed too.

## 2 Formulation

We consider a flow between vertical plates  $y^* = \pm L$  that depends on time  $t^*$  and coordinate  $y^*$  only and is driven by constant pressure gradient  $\partial p / \partial z^*$  in the vertical direction in addition to the hydrostatic pressure. The momentum and energy equations, under the well-accepted Boussinesq approximation, are [10]

$$\rho \frac{\partial W}{\partial t^*} = \mu \frac{\partial^2 W}{\partial y^{*2}} - \frac{\partial p}{\partial z^*} + \rho g \beta (T - T_a), \quad (1)$$

$$\rho c \frac{\partial T}{\partial t^*} = k \frac{\partial^2 T}{\partial y^{*2}} + \mu \left( \frac{\partial W}{\partial y^*} \right)^2. \quad (2)$$

The boundary conditions are

$$W = 0, \quad T = T_a \quad \text{at } y^* = \pm L. \quad (3)$$

Here  $\mu$  is the viscosity of the fluid,  $g$  is the gravitational acceleration,  $\beta$  is the coefficient of thermal expansion,  $k$  is the thermal diffusivity,  $c$  is the specific heat,  $T$  is the temperature,  $T_a$  is the same ambient temperature on the walls, and  $\rho$  is the density at  $T_a$ .

\* Corresponding author Email: milan@math.msu.edu

Scaling

$$y = \frac{y^*}{L}, \quad t = t^* \frac{\mu}{L^2 \rho}, \quad w = W \frac{\rho g \beta L^2}{k}, \quad \theta = (T - T_a) \frac{(\rho g \beta L^2)^2}{k \mu} \quad (4)$$

gives our main equations

$$\frac{\partial w}{\partial t} = \frac{\partial^2 w}{\partial y^2} - \Pi + \theta, \quad (5)$$

$$\text{Pr} \frac{\partial \theta}{\partial t} = \frac{\partial^2 \theta}{\partial y^2} + \left( \frac{\partial w}{\partial y} \right)^2, \quad (6)$$

$$w = 0, \quad \theta = 0 \quad \text{at } y = \pm 1 \quad (7)$$

where the Prandtl number  $\text{Pr}$  and the scaled pressure gradient  $\Pi$  are given by

$$\text{Pr} = \frac{c \mu}{k}, \quad \Pi = \frac{\partial p}{\partial z^*} \frac{\rho g \beta L^4}{k \mu}. \quad (8)$$

The symmetric stationary solutions of (5), (6), (7) satisfy

$$0 = w'' - \Pi + \theta, \quad (9)$$

$$0 = \theta'' + (w')^2, \quad (10)$$

$$w' = 0, \quad \theta' = 0 \quad \text{at } y = 0, \quad w = 0, \quad \theta = 0 \quad \text{at } y = 1. \quad (11)$$

Solutions are shown on Figs. 1 and 2. For each solution we give  $\Pi$ ,  $w(0)$ ,  $\theta(0)$  so that readers can use their own software to solve Eqs. (9), (10) as an initial value problem. The completely passive convection solution [6] is at  $\Pi = 0$  on the upper branch (point F) on Fig. 2 and has  $w(0) = 6.111400215$ ,  $\theta(0) = 13.15510836$ .

This  $w$  and  $\Pi$  are related to  $u$  and  $\varepsilon$  in [1] (symmetric heating case) as follows

$$w(y) = \frac{\varepsilon}{16} u\left(\frac{y}{4}\right), \quad \Pi = -\frac{3\varepsilon}{16}. \quad (12)$$

The flows presented in [1] for  $\varepsilon = \pm 12$  ( $\Pi = \mp 2.25$ ) correspond to points B and C on the lower branch on Fig. 2.

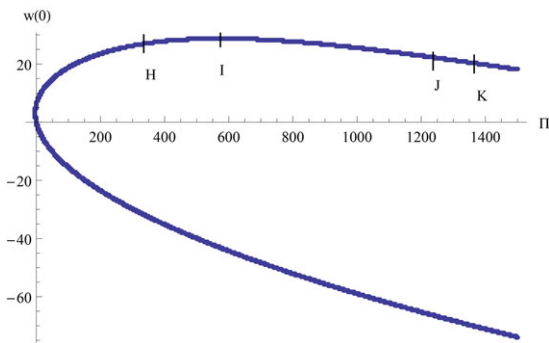


**Fig. 1** Stationary solutions. H,J,K represent flows studied in [2]. Maximum  $\Xi$  (Eq. (14)) occurs at H,  $\Xi = 20$  at J and  $\Xi = -20$  at K. Maximum  $w(0) = 28.77154133$  occurs at I when  $\Pi = 574.025$  and  $\theta(0) = 704.777$ .

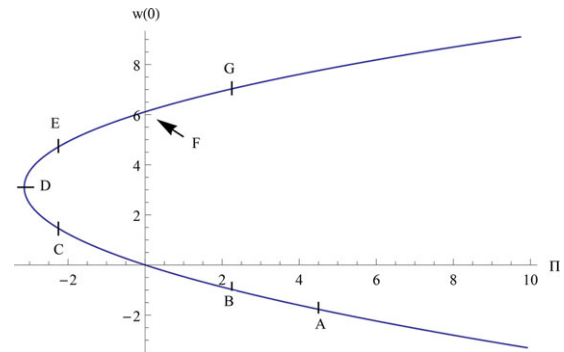


**Fig. 2** Stationary solutions near the turning point D at  $\Pi = -3.13764829$ ,  $w(0) = 3.09853$ ,  $\theta(0) = 3.28514$ . Solutions obtained in [1] are at B and C ( $\Pi = \pm 2.25$ ). The completely passive convection solution [6] is at F.

Our stationary solutions  $w$  are related also to  $u$  and  $\Xi$  in [2] as follows

$$w(y) = \frac{\Xi}{16} u(y). \quad (13)$$

Given  $w$  define

$$\Xi = 16 \int_0^1 w(y) dy \quad (14)$$

and use above (13) to obtain  $u$  as in [2].  $\Xi$  represents (eight times) the total flow rate per width. The maximum value of  $\Xi = 228.12869$  agrees with the value given in [2] and it occurs at  $\Pi = 334.88$ ,  $w(0) = 26.961$ ,  $\theta(0) = 430.03$ .  $\Xi$  monotonically decreases toward  $-\infty$  as we move away from the maximum value at the point H on Fig. 1 in either direction. So, for each  $\Xi$  below the maximum value we can find dual solutions [2]: one to the right of H and one to the left of H that have the same  $\Xi$ . In [2] detailed profiles of two dual solutions at  $\Xi = \pm 20$  are presented. The solutions with flow reversals occur at points J and K on Fig. 1 and their duals are near points C and A, respectively, on Fig. 2. Note, that the dual of the trivial solution ( $\Xi = 0$ ) is between J and K.

It will be shown in the next section that solutions on the upper branch, starting at the turning point D, are unstable. However, Fig. 3 shows that there are no obvious changes in graphs of  $w$  and  $\theta$  during the transition from the trivial solution to the completely passive natural convection solution. (9), (10), (11) imply that  $w'' < 0$  when  $\Pi < 0$ . There are no inflection points in the velocity graphs. The inflection points start appearing at exactly  $\Pi > 0$  on the upper branch and lead to flow reversal at large  $\Pi$ . Rayleigh's necessary condition for instability of shear flow states that there must exist a point of inflection in the velocity profile for instability to occur. This condition is often quoted but it is derived for inviscid flows with no heat conduction.

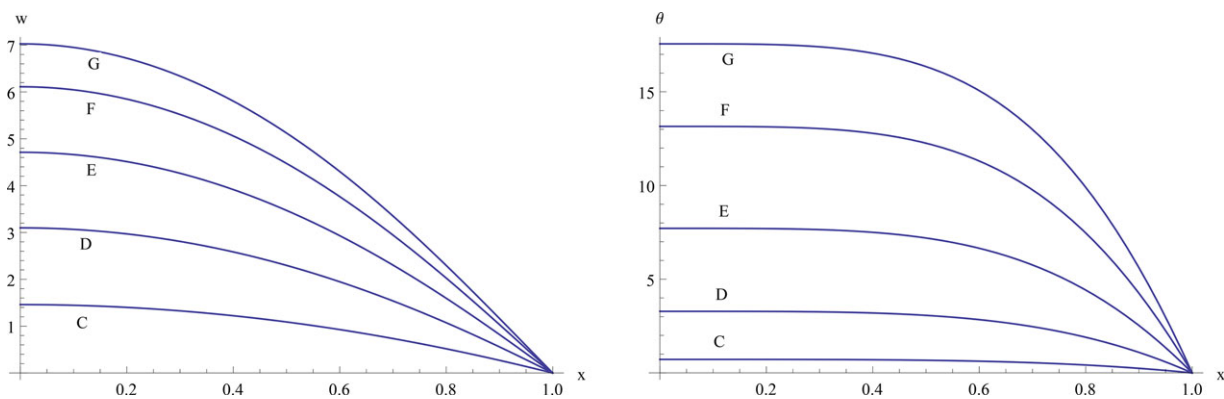


**Fig. 3** Velocity and temperature profiles during the transition from the trivial solution to the completely passive convection solution (F). Flows above D are unstable, flows below D are stable.

### 3 Stability

Let  $w, \theta$  be even and satisfy (9), (10), (11) for some  $\Pi$ . If perturbations

$$w(y) + u_1(y, t), \quad \theta(y) + u_2(y, t)$$

satisfy Eqs. (5), (6), (7) then

$$\frac{\partial u_1}{\partial t} = \frac{\partial^2 u_1}{\partial y^2} + u_2, \tag{15}$$

$$\text{Pr} \frac{\partial u_2}{\partial t} = \frac{\partial^2 u_2}{\partial y^2} + 2w' \frac{\partial u_1}{\partial y} + \left( \frac{\partial u_1}{\partial y} \right)^2, \tag{16}$$

$$u_1 = 0, \quad u_2 = 0 \quad \text{at } y = \pm 1. \tag{17}$$

This system can be considered as an abstract evolution equation

$$\frac{\partial u}{\partial t} + Au = f(u) \tag{18}$$

of  $u = (u_1, u_2)$  in  $(L^2(-1, 1))^2$  where the linear operator  $A$  is given by

$$(Au)_1 = -u_1'' - u_2, \quad (Au)_2 = (-u_2'' - 2w'u_1')/\text{Pr} \tag{19}$$

with the domain  $D(A) = (W_0^1(-1, 1) \cap W^2(-1, 1))^2$  and

$$f(u)_1 = 0, \quad f(u)_2 = (u_1')^2/\text{Pr}. \tag{20}$$

One can prove that (18) is a semilinear parabolic equation [5] and that  $A$  has compact resolvent. Hence the well known stability theory for semilinear parabolic equations, see for example [5], can be applied to show that (nonlinear) stability of stationary solutions  $w, \theta$  is determined by the eigenvalues of  $A$ .  $-\lambda$  is an eigenvalue of  $A$  iff there exists a nontrivial solution of

$$\lambda v = v'' + \tau, \quad (21)$$

$$\text{Pr} \lambda \tau = \tau'' + 2w'v', \quad (22)$$

$$v = \tau = 0 \quad \text{at} \quad y = \pm 1. \quad (23)$$

In this notation, if every eigenvalue  $\lambda$  has negative real part then all small perturbations of the stationary solution decay (p. 265 in [5]). If on the other hand at least one eigenvalue has positive real part then one can find arbitrarily small perturbations of the stationary solution that eventually become larger than a fixed threshold (p. 266 in [5]).

The obvious central difference approximations were used to discretize (21), (22) and then the eigenvalues of the corresponding matrix were calculated. Richardson extrapolation, using two discretizations, was used to improve accuracy. For reference values see (24), (28).

The trivial solution  $w = \theta = \Pi = 0$  of (9), (10), (11) is stable because the eigenvalues are equal to

$$-(n\pi/2)^2, \quad -(n\pi/2)^2/\text{Pr} \quad \text{where } n = 1, 2, \dots \quad (24)$$

When  $1/4 < \text{Pr} < 4$  the leading eigenvalues are  $-(\pi/2)^2$  and  $-(\pi/2)^2/\text{Pr}$ . As  $w(0)$  decreases from 0, i.e. moving to the right of 0 on the lower branch of Fig. 2, they merge and then form a complex conjugate pair with slowly varying real part, see Fig. 4. More specifically, when  $\text{Pr} = 2$  the real part of the leading eigenvalue at  $w(0) = -2$  equals  $-1.85$  and it increases to  $-1.34$  at  $w(0) = -71$  ( $\Pi = 1400$ ). When  $\text{Pr} = 1$ , the merge point is simply at  $w(0) = 0$ , but otherwise the eigenvalue graph looks very similar to Fig. 4.

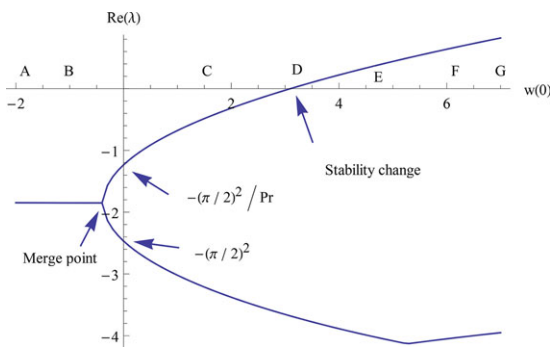


**Fig. 4** Real parts of two of the largest eigenvalues when  $\text{Pr} = 2$ .

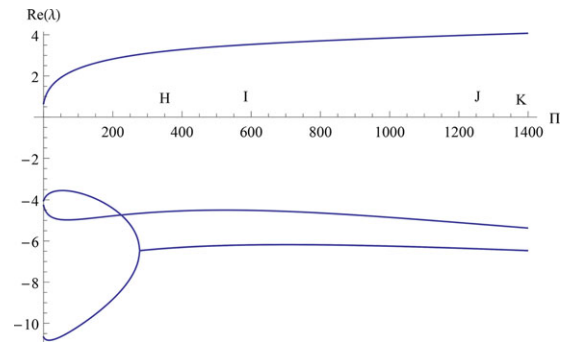


**Fig. 5** Real parts of four of the largest eigenvalues when  $\text{Pr} = 2$  on the upper branch of Fig. 1.

On the other hand as  $w(0)$  increases, i.e. moving up from 0 on Fig. 2, the eigenvalues separate more and the leading one changes the sign at exactly the turning point D. See Fig. 4. Therefore the solutions on the lower branch (Figs. 1, 2) are stable.

To show that stability changes at exactly the turning point D consider the solutions  $w, \theta$  of (9), (10), (11) as a function of  $s = w(0)$ , i.e.

$$w = w(s, y), \quad \theta = \theta(s, y), \quad \Pi = \Pi(s) \quad w(s, 0) = s. \quad (25)$$

Taking derivative with respect to  $s$  of (9), (10) gives

$$0 = \frac{\partial^2 w_s}{\partial y^2} - \Pi_s + \theta_s, \quad (26)$$

$$0 = \frac{\partial^2 \theta_s}{\partial y^2} + 2 \frac{\partial w}{\partial y} \frac{\partial w_s}{\partial y} \quad (27)$$

where  $w_s = \partial w / \partial s$ ,  $\theta_s = \partial \theta / \partial s$ , and  $\Pi_s = \partial \Pi / \partial s$ . At the turning point D we have that  $\Pi_s = 0$  hence Eqs. (21), (22) imply that  $w_s$  and  $\theta_s$  are eigenfunctions with eigenvalue  $\lambda = 0$ . This proves that one eigenvalue, as a function of  $s$ , has a zero at D. Generically one would expect that the derivative of the eigenvalue with respect to  $s$  is nonzero at D and hence the

eigenvalue changes sign at D. This can be proved, independently of actual computation of the eigenvalues, see for example [7]. However, direct computation of the eigenvalues, as done here is much simpler. This of course does not exclude the possibility that another eigenvalue changes sign before the turning point D. (24) actually implies that when  $Pr$  is large there are a lot of eigenvalues crowded between 0 and  $-(\pi/2)^2$  and one may speculate that perhaps one of them would cross 0 before the turning point D, however, this was not observed numerically. In the range  $0.001 < Pr < 10,000$  the crossover was observed only at the turning point D.

As  $w(0)$  increases past the turning point D, i.e. moving onto the upper branch on Figs. 1 and 2, the leading eigenvalue becomes positive, Fig. 4. The two largest eigenvalues for the completely passive natural convection at  $Pr = 2$  are

$$0.6591670, \quad -4.038936. \quad (28)$$

The largest eigenvalue in case of the completely passive natural convection flow is positive and

$$\lim_{Pr \rightarrow 0} \lambda = \lim_{Pr \rightarrow \infty} \lambda * Pr = 2.333... \quad (29)$$

Hence the completely passive natural convection is an unstable flow.

Since maximum  $w(0)$  is reached on the upper branch it makes more sense to use  $\Pi$  as a parameter in presentation of eigenvalues on the on the upper branch. See Fig. 5. The leading eigenvalue is simply increasing with  $\Pi$  which makes all stationary solutions on the upper branch in Figs. 1, 2 unstable. Figure 5 hints at an interesting behavior near  $\Pi = 0$ , but this is an artifact of the fact that all eigenvalue branches need to turn at the turning point D. In particular, the first (top) and the third eigenvalue near  $\Pi = 0$  on Fig. 5 turn near  $\Pi = -3$  and are heading toward the merge point near  $\Pi = 1$  on the lower branch on Fig. 2.

Let us now look at stability of dual solutions in [2]. Since the maximum value of  $\Xi$  occurs on the upper branch on Fig. 1 and since one of the dual solutions is to the right of it this solution has to be unstable. So, one of the dual solutions is always unstable. At the turning point D the total flow rate equals  $\Xi_T = 32.707$ . Since  $\Xi$  monotonically decreases toward  $-\infty$  as we move away from the maximum value at the point H on Fig. 1 in either direction we have that both dual solutions are unstable when  $\Xi > \Xi_T$  and that one of the dual solutions is stable when  $\Xi < \Xi_T$ . In particular, the solutions at points J and K on Fig. 1 are unstable, but their duals are stable because their  $\Xi < \Xi_T$ . The completely passive natural convection and its dual have  $\Xi = 8 * 7.972440121 > \Xi_T$  and are both unstable. While stationary solutions do not depend on the choice of reference temperature [2] the point of stability change may depend on it and hence the value of  $\Xi_T$  may change if average temperature is used in place of  $T_a$  in Eq. (1), but its derivation would not change.

## References

- [1] A. Barletta, Laminar mixed convection with viscous dissipation in a vertical channel, *Int. J. Heat Mass Trans.* **41**, 3501–3513 (1998).
- [2] A. Barletta, E. Magyari, and B. Keller, Dual mixed convection flows in a vertical channel, *Int. J. Heat and Mass Transf.* **48**, 4835–4845 (2005).
- [3] A. Barletta, S. Lazzari, and E. Magyari, Buoyant Poiseuille-Couette flow with viscous dissipation in a vertical channel, *Z. Angew. Math. Phys.* **59**, 1039–1056 (2008).
- [4] A. Barletta and E. Zanchini, On the choice of the reference temperature for fully developed mixed convection in a vertical channel, *Int. J. Heat Mass Trans.* **42**, 3169–3181 (1999).
- [5] M. Miklavčič, *Applied Functional Analysis and Partial Differential Equations* (World Scientific Publishing Co. Inc., River Edge, NJ, 1998).
- [6] M. Miklavčič and C. Y. Wang, Completely passive natural convection, *Z. Angew. Math. Mech.* **91**, 601–606 (2011).
- [7] M. Miklavčič, Instability of viscous flows over a shrinking sheet, *Quart. Appl. Math.* **72**, 363–371 (2014).
- [8] M. Miklavčič and C. Y. Wang, Viscous flow due to a shrinking sheet, *Quart. Appl. Math.* **64**, 283–290 (2006).
- [9] W. Schneider, Comments on M. Miklavčič and C. Y. Wang, Completely passive natural convection, *ZAMM* **91**(7), 601–606 (2011)], *Z. Angew. Math. Mech.* **91** (2011), 1002–1004.
- [10] F. M. White, *Viscous Fluid Flow*, 3rd edition (McGraw-Hill, Boston, 2006).
- [11] G. Wilks and J. S. Barnley, Dual solutions in mixed convection, *Proc. Roy. Soc. Edinburgh A* **87**, 349–358 (1981).